

## VIRTUAL SIMULATION OF SHAPE GENERATION OF HOMEOSTATIC SHELL MODELS

Patricia M. Bellés<sup>1,2</sup>, Marta B. Rosales<sup>1,3</sup>, and Miguel A. Conca<sup>4</sup>

<sup>1</sup>Department of Engineering, Universidad Nacional del Sur. Alem 1253, 8000 Bahía Blanca,  
Argentina. e-mail: [pbelles@criba.edu.ar](mailto:pbelles@criba.edu.ar), [mrosales@criba.edu.ar](mailto:mrosales@criba.edu.ar)

<sup>2</sup>CIC, Buenos Aires, Argentina

<sup>3</sup>CONICET, Argentina

<sup>4</sup>Previous CIC scholar

**Keywords:** virtual experiment, homeostatic models, finite elements, structural shell

**Abstract.** This paper deals with the shape generation of structural shells within the field of Conceptual Design. A virtual simulation of previous experiments on physical “homeostatic” models, carried out by other authors, is herein presented. The physical experiments were based on the biological principle of “Homeostasis”: when an external agent attacks the structure, the latter defends itself intelligently to recover its bearing capacity. Heat is the external agent used to cause the model material degradation. Thus the model adopts a more appropriate structural shape in order to continue resisting loads. The virtual simulation is performed using a finite element software with a thermal elasto-plastic material model. In particular, Polymethyl Methacrylate (PMMA) is considered. Comparisons between the shapes found with the physical and virtual experiments are presented. Additionally, the obtained geometry is employed as the shape of a concrete shell and a stress analysis is presented. A quasi-membranal behavior is shown.

## 1 INTRODUCTION

The aim of the *Homeostatic Model Technique* (HMT) is the conceptual design of surface structures. This technique, introduced by Andrés (1989) and based on Gaudi's funicular technique, consists in a simultaneous action of loads and temperature over a plane plate of thermoplastic material. As a consequence of the mechanical properties degradation due to the heating the material undergoes a deformation adopting a funicular shape that is under pure tensile stress in the case of dead loads. After that the deformed model is cooled. It is then placed in an inverted position yielding an “antifunicular” shell that is subjected to compressive stresses (a quasi-membranal state) under the action of self weight.

Several articles have been published by Andrés and co-authors —Andrés (1989), Andrés (1998), Andrés and Ortega (1991), Andrés and Ortega (1993), Andrés *et al.* (1994), Andrés *et al.* (1998)— describing the basic ideas of HMT and verifying its reliability as a tool for the design of structural shapes. Similar results on shapes generation have been reported regarding concrete shell shapes also found using finite element method with progressive load increments (Fernández *et al.* (2002) and Moisset de Espanes *et al.* (2000)).

The main purpose of the present study is to perform a virtual simulation of the experimental work based on the simultaneous action of heat and loads over a thermo-plastic shell. The finite element method (FEM) is used with this purpose, and additionally to analyze the mechanical behavior of a hypothetical concrete shell based on the homeostatic shape.

Briefly, the process of the (experimental) model generation may be described as follows. A plate-boundary restrictions-load set is introduced in a oven that is heated until the deformations are stabilized. Then the deformed model is cooled. The resulting shape is then inverted and used as the model of a concrete shell roof.

## 2 GEOMETRY GENERATION: FINITE ELEMENT MODEL

The first part of this work deals with the simulation of the HMT using MEF. The tool Mechanical Event Simulation (MES) of the nonlinear processor of Algor (Algor software, 2004) is used. The experimental test is reproduced from a model of a thermoplastic material with the same boundary conditions and loading as the test carried out in the oven.

### 2.1 Experimental model, boundary conditions and loading.

The experimental model is a square plate of Polymethyl Methacrylate (PMMA) supported at its four corners. The plate is 0.36m of side and 2.4 mm of thickness. A distributed load is applied by means of a load pad (Figure 1) that is equivalent to the structural design load. Such pad is constructed by sticking small metal pieces to a polystyrene sheet. In this way the dead load is distributed uniformly over the surface without offering resistance to deformation.

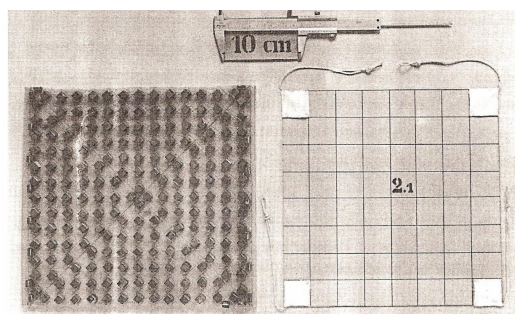


Figure 1. Photograph of the load pad applied over the experimental plate.

The plate is hung from the four corners by a system of four pulleys with counterweights that equilibrate the model weight. In Figure 2 a photograph (Andrés and Ortega, 1993) of a typical set up (although a different support case) of the test can be observed.



Figure 2. Experimental plate before deformation (Andrés and Ortega, 1993).

The geometry of the finite element model is a square prism of the same dimensions that the physical model. Despite the slenderness, a tridimensional model with brick elements was employed since the thermoplastic material model is only available for this type of element. The plate external boundaries are modeled with supports at the four corners that allow displacements within the plate plane but restrict the transverse motion.

The load pad is taken into account by assuming a fictitious density of  $7900 \text{ g/m}^3$ , that includes the dead load and the surface load.

## 2.2 Material model

In the problem under study, the material characterization is, without doubt, the issue with more uncertainties due to the lack of information of some of the properties of the materials used in the physical test.

The tool Accupac/NLM with the material model “Thermal elasto-plastic” requires the definition of the coefficient of thermal expansion, the Young’s modulus, the Poisson’s ratio, the uniaxial yield stress and the strain hardening as functions of temperature. This model is appropriate when stresses can exceed the yield stress and the mechanical behavior is affected by temperature changes. Typical applications of this model are metals and polymeric materials.

The thermoplastic material model is represented by a bi-linear curve. The mechanical behavior of thermoplastic in monotonic loading is characterized by an initial linear elastic response, followed by distributed yielding, large scale plastic flow, and gradual strain

stiffening until failure is initiated.

It has an elastic modulus, which describes the stress rate from 0 to the yield strain, then uses a strain hardening modulus to describe linearly the stress rate from the yield strain to infinite strain. The program requires to define indices having temperature data that brackets the temperature range that may exist in the model. (see Table 1)

Index	Temp. (°C)	Elastic Modulus (N/m <sup>2</sup> )	Poisson's Coefficient	Thermal expansion Coefficient (1/°C)	Uniaxial yield stress (N/m <sup>2</sup> )	Strain hardening modulus (N/m <sup>2</sup> )
1	0	3.2e9	0.3	6.0e-5	6.4e7	5.0e7
2	20	3.0e9	0.313	6.5e-5	5.76e7	4.0e7
3	40	2.6e9	0.325	6.7e-5	4.48e7	3.0e7
4	60	1.9e9	0.345	8.2e-5	3.62e7	2.0e7
5	70	1.5e9	0.358	8.4e-5	3.18e7	1.5e7
6	80	1.3e9	0.37	8.6e-5	1.7e7	1.0e7
7	100	4.0e8	0.42	1.4e-4	2.0e6	5.0e6
8	120	4.0e8	0.49	1.95e-4	2.0e6	0
9	140	4.0e8	0.49	2.0e-4	2.0e6	0

Table 1. Properties of PMMA as a function of temperature.

Despite research efforts, the physical origin of strain hardening is not fully understood ([van Melick et al., 2003](#)). Commercial PMMA always contains some copolymer as ethyl acrylate (EA) for example, to facilitate processing. Curves ([Kierkels et al. 2005](#)) that shows how strain hardening decreases with temperature for 4 types of PMMA with different contents of EA are shown in Figure 3. In the present application an average value from this curves was adopted.

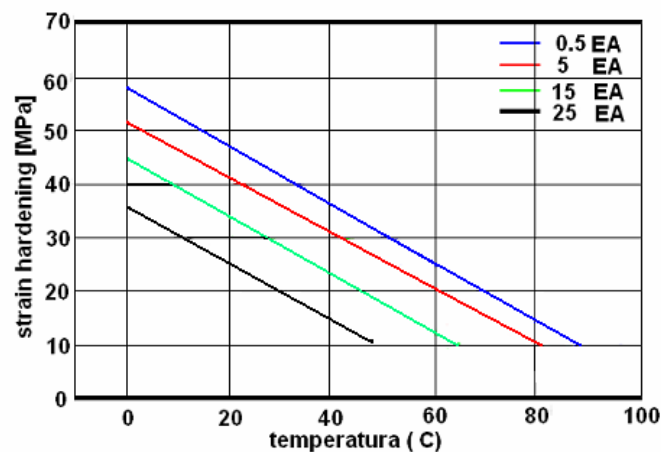


Figure 3. Strain hardening of PMMA as a function of temperature.

Other characteristic values were obtained from the available literature ([Oberbach, 1978](#), [Ortega, 1998](#) and [Paloto and Ortega, 1998](#)): variation with temperature of the elastic modulus (Figure 4), Poisson's coefficient (Figure 5), and coefficient of thermal expansion (Figure 6).

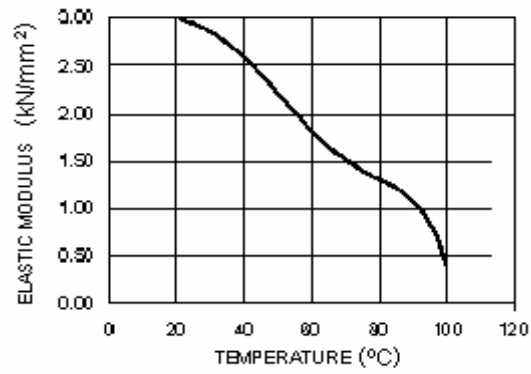


Figure 4. Elastic modulus of PMMA.

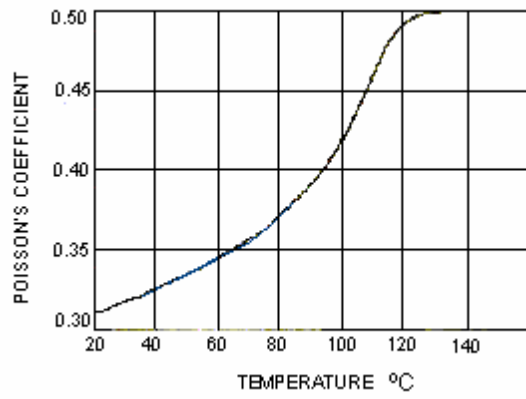


Figure 5. Poisson's coefficient of PMMA.

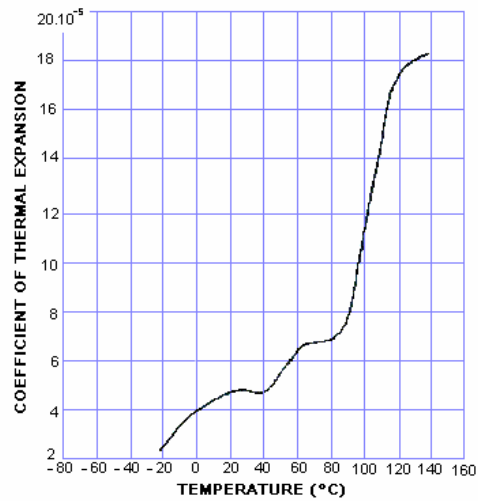


Figure 6. Coefficient of thermal expansion of PMMA.

### 2.3 Simulation of the heating and cooling process.

In the physical experiment the plate is introduced in the oven and heated uniformly until temperature reaches 140°C approximately. Then it is cooled and at this stage the original stiffness is recovered.

In the finite element model the heating and cooling process is introduced by means of a multiplier curve, shown in Figure 7, that is applied on an initial unit temperature uniform over the plate. This action is activated once the effect of the gravitational loads is stabilized.

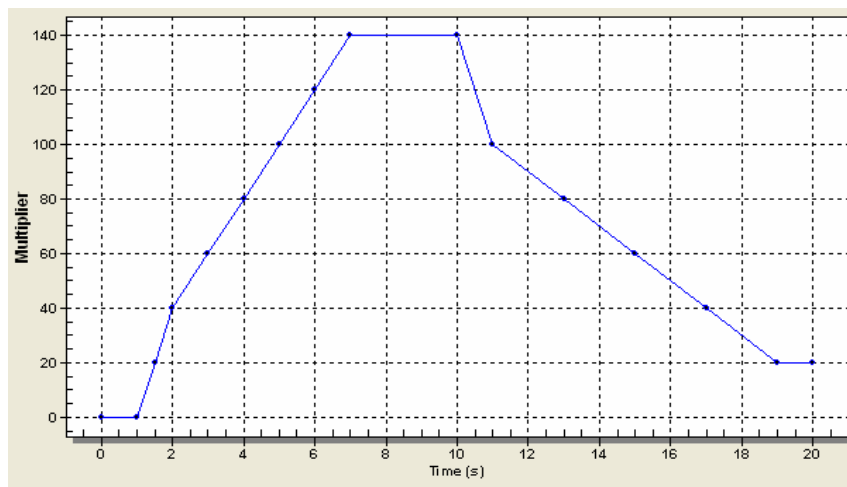


Figure 7. Temperature variation in the heating-cooling process (MES).

### 3 COMPARISON BETWEEN THE MEF MODEL AND PHYSICAL MODEL

Figure 8 depicts the deformed plate resulting from the numerical simulation.

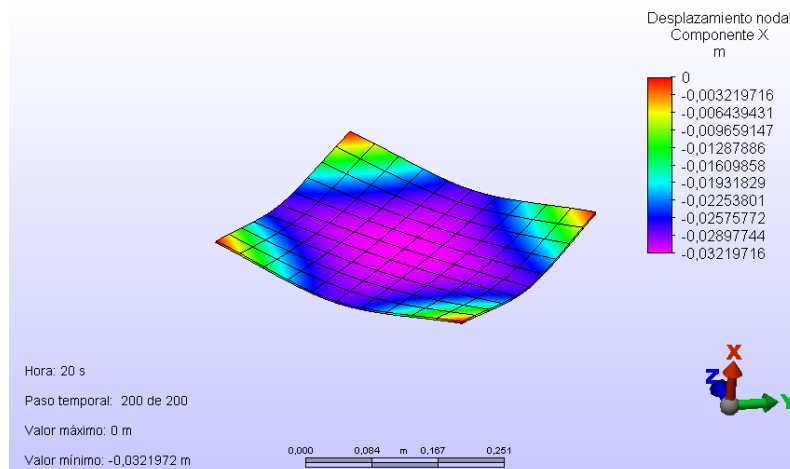


Figure 8. Transverse deformation of the MEF model.

The displacements suffered by the plate transversely to its plane are displayed in the legend at the upper-right corner of Figure 8. The maximum value attained at the center of the plate reaches 32.2mm.

The plot of Figure 9 shows the variation of the displacements at the central node of the plate (green) and at midspan of one boundary (blue) with time. It can be observed that the displacements are stabilized beyond 12 seconds.

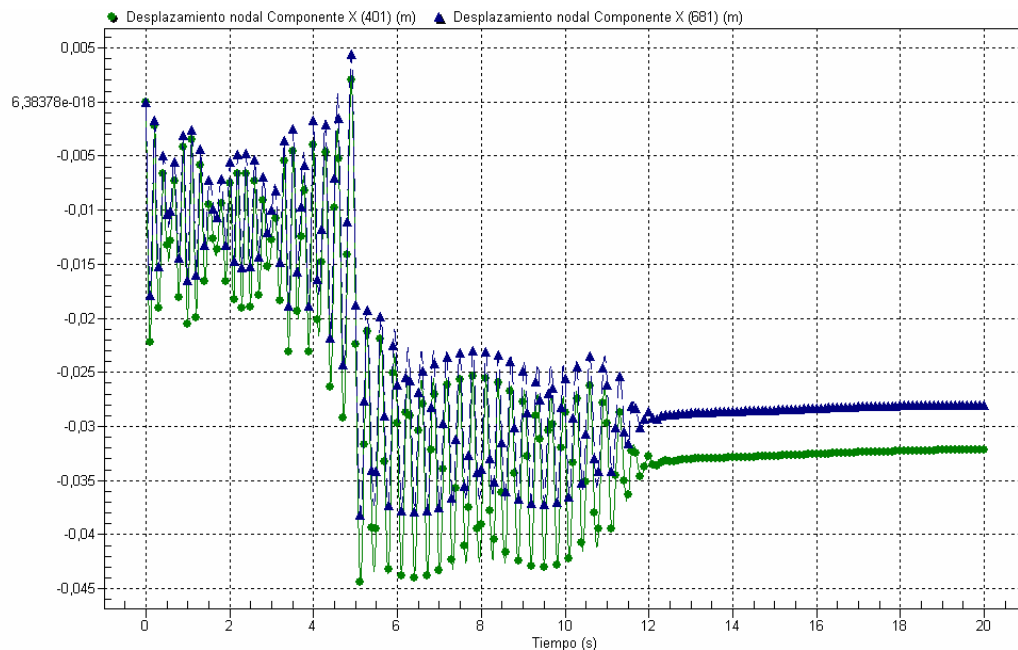


Figure 9. Displacements at the central node of the plate (green) and central node of a boundary (blue).

The photograph shown in Figure 10 (from <http://bc.uns.edu.ar/andres/teoria.html>) was taken to a deformed experimental model once the test is finished.



Figure 10. Physical model after the test.

Figure 11 depicts the final deformation curves of the numerical model (continuous lines) compared with the deformation obtained in the physical experiment (dashed lines). The reference system origin is located at the midpoint of the plate, with ten divisions on each side.

It may be observed that both models behave similarly. The agreement is better in the boundaries (red line) with larger discrepancies towards the center (black lines). Such differences are due mainly to the different modeling of the supports in the physical and numerical models and in the uncertainties of the material model.

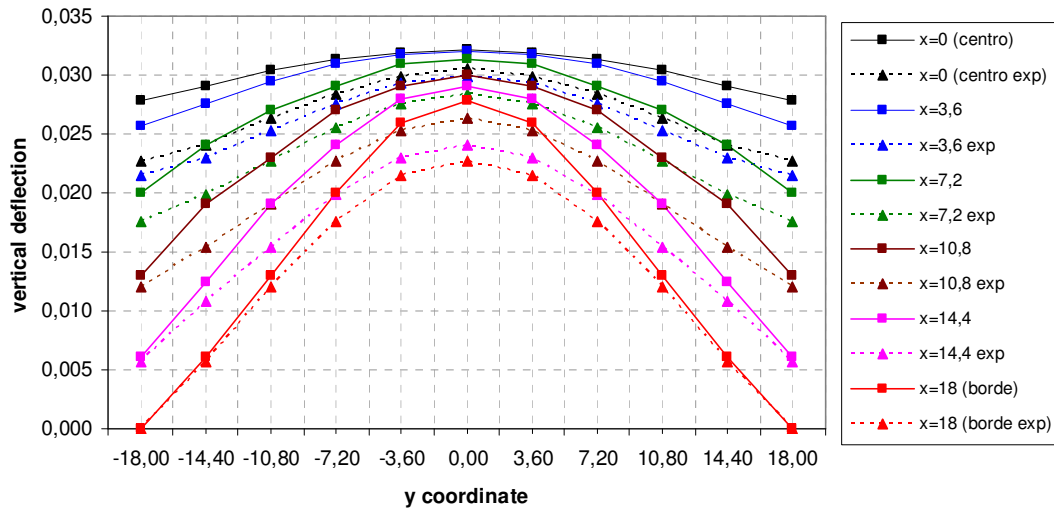


Figure 11. Transverse displacement across the plate. Physical model (dashed lines) and numerical model (continuous lines).

Additionally, the influence of the material mass density in the deformations was studied. Figure 12 depicts the relationship density vs. maximum displacement at the center of the plate, showing the sensibility of the model to density variations. As mentioned before, in this problem the density was assumed to be 7900 g/m<sup>3</sup> including the dead and live loads.

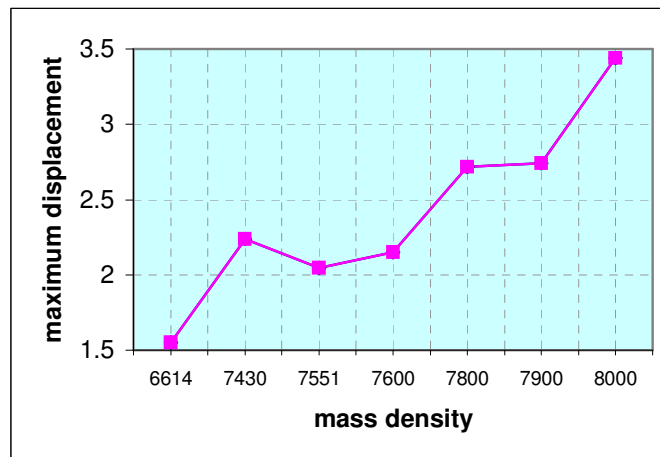


Figure 12. Maximum displacement variation with the mass density.

#### 4 CONCRETE STRUCTURAL SHELL

The shape obtained from both the physical and the numerical experiment yields, when reversed, the “antifunicular” of gravitational loads. A structural shell constructed with this shape will behave in a quasi-membranal state under such loads.

In order to verify this fact, in what follows the performance of a numerical model of a concrete structural shell with the above generated shape is studied. The next properties are assumed: mass density= $2404.6 \text{ g/m}^3$ , Young's modulus  $E=2.0684e10 \text{ N/m}^2$ , Poisson's coefficient  $\nu=0.15$ .

As before, brick elements were employed in the tridimensional model. The above generated geometry is captured by the program (a capability of Algor software) and then uniformly re-scaled in an appropriate manner. In this case, it was assumed that the shell should span a square of 20 m side, resulting a thickness of 0.143 m.

The model is restricted by clamping its four corners and subjected to self weight load. From the static analysis a maximum displacement of 18.8mm is obtained at the center of the plate as may be seen in Figure 13.

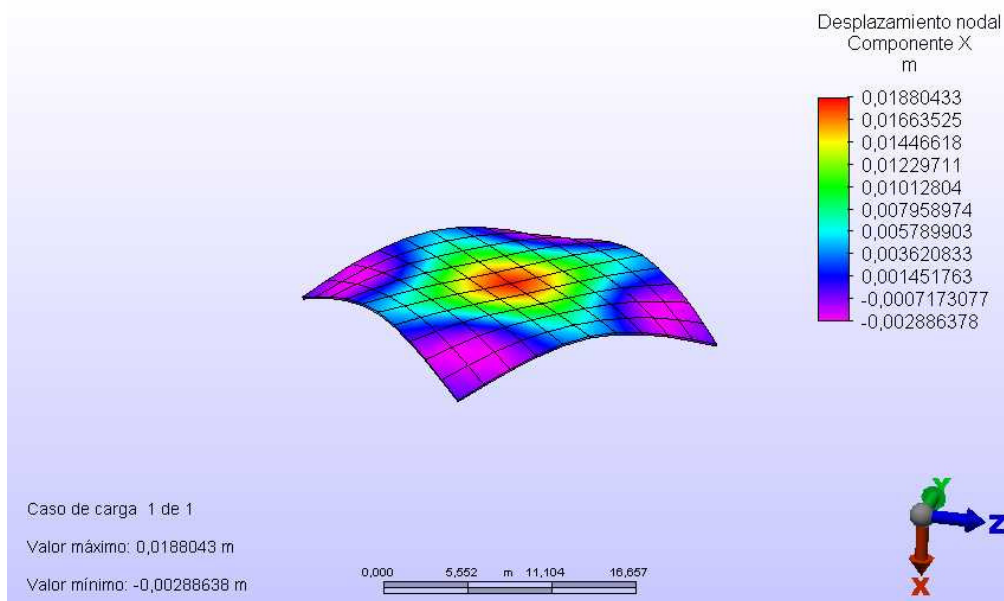


Figure 13 Vertical displacements of the concrete shell under self weight load.

The maximum and minimum stresses are shown in Figures 14 and 15. The extreme values are 2.1 Mpa (tensile stress, maximum principal stress) and -8.78 Mpa (compression, minimum principal stress). Both values are below the admissible limits assumed for this material (2.1 Mpa for tensile stress and 21 Mpa for compression).

Figure 16 depicts the Von Mises stresses that reach a maximum of 7.4 Mpa (the limit stress for concrete is 15 Mpa )

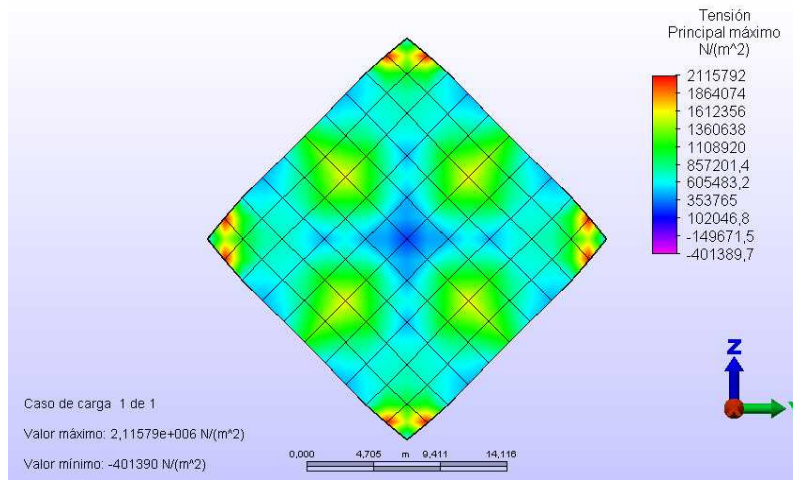


Figure 14. Maximum principal stresses in the concrete structural shell.

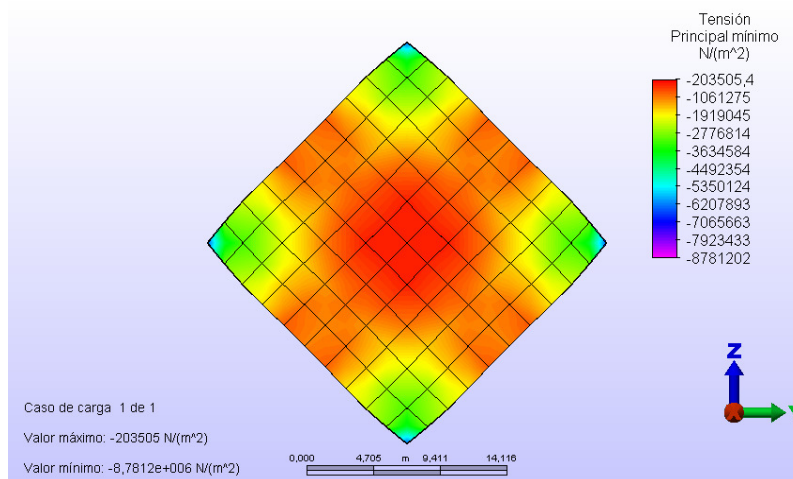


Figure 15. Minimum principal stresses in the concrete structural shell.

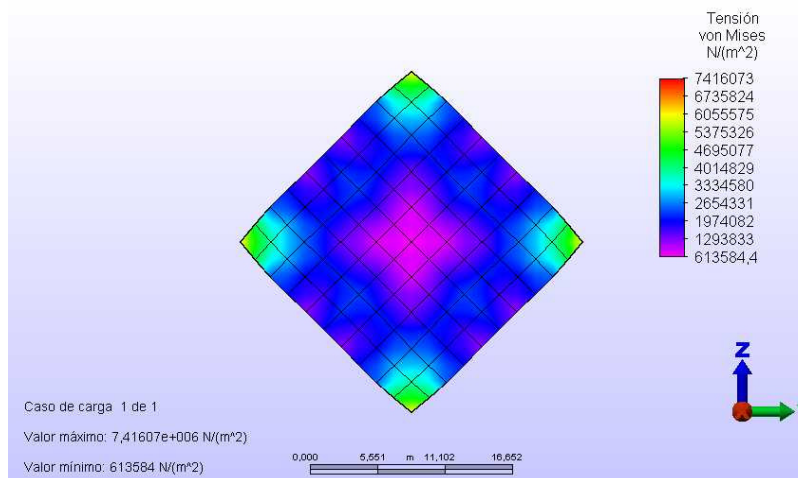


Figure 16. Von Mises stresses in the concrete structural shell.

It should be noted that this example is only a preliminar model to show the software capability to capture the geometry of the previous homeostatic model. The brick element herein used is the most simple one (isotropic, without intermediate nodes, with second order integration). Obviously higher order element could be used and are available in the software. Also more elements along the thickness should be employed. However this study would be beyond the primary scope of this work.

## 5 CONCLUSIONS

This paper dealt with the shape generation of structural shells within the field of Conceptual Design. A virtual simulation of previous experiments on physical “homeostatic” models, carried out by other authors, was herein presented.

From a numerical model (finite elements) with analogous conditions to the physical test, the homeostatic shape is generated. It may be concluded that the laboratory test results were adequately reproduced.

The main overcoming in the construction of the finite element model arose from the difficulty of characterizing the thermoplastic model used in the physical test, in this case PMMA (Polymethyl Methacrylate) regarding the constitutive properties. The employed software requires of the use of brick elements for this material model despite dealing with thin plate/shell.

The analysis of the stresses and deformations of a concrete shell with the antifunicular shape found with the HMT allows the verification of the quasi-membranal behavior.

## 6 ACKNOWLEDGMENTS

The authors want to acknowledge the information and comments given by Professors O. Andres and N. Ortega. This study has been partially supported by a grant from SGCyT of the Universidad Nacional del Sur, Argentina.

## 7 REFERENCES

- Algor Software. Versión 16.00, 2004. Pittsburg, USA.
- Andrés O.A., Homeostatic Models for Shell Roofs Design, Proc. IASS Congress, CEDEX Laboratorio Central de Estructuras y Materiales, Vol. 1, Madrid, 1989.
- Andrés, O.A. Modelos homeostáticos para diseño de cubiertas laminares, Memorias de las VIII Jornadas Argentinas de Ingeniería Estructural, Buenos Aires, 1998.
- Andrés, O.A., Ortega, N.F. Experimental Design of Free Form Shell Roofs. Proc. IASS Symposium, Kuntsaademiets Forlag Aritetsolen, Vol. II, p. 69, Copenhagen, 1991.
- Andrés, O.A., Ortega, N.F. Extensión de la técnica funicular de Gaudí a la concepción y génesis de superficies estructurales. (Primer Premio del concurso Iberoamericano de informes 1992, Arquitectura e Ingeniería en Iberoamérica: hombre, naturaleza y ciudad). Informes de la Construcción, Vol. 44 n° 424, marzo/abril 1993.
- Andrés, O.A., Ortega, N.F., Schiratti C. Comparison of two different models of a shell roof. ASCE Structures Congress XII – IASS International Symposium '94. Atlanta, Georgia, USA. 24 al 28 de abril de 1994.
- Andrés, O.A., Ortega, N.F., Paloto J.C. The homeostatic model as a total model. Proc. IASS

- Symposium on lightweight structures in architecture. Engineering and construction, LSA 98, Vol.2, Sydney, 1998.
- Fernández M.C., Ruata M.E., Moisset de Espanes D. Capacidad sismorresistente de estructuras laminares antifuniculares. VII Jornadas de Ingeniería Estructural, 4 al 6 de set. 2002, Rosario, Argentina, 2002.
- Kierkels, J.T., Leblanc, T., Goossens, J.G., Goavert, L.E., Meijer H.E., Influence of network density on the strain hardening of PMMA copolymers. Technische Universiteit eindhoven. Department of mechanical engineering, 2005.
- Moisset de Espanes D., Fernández M.C., Ruata M.E., Efectos del viento y seguridad al pandeo de estructuras laminares antifuniculares. Instituto de la Construcción y Gerencia, Lima, Perú. <http://www.construccion.org.pe/>
- Oberbach, K., "Plásticos. Valores característicos para el diseño de estructuras". Ed. AmericaLee, 1978, Buenos Aires.
- Ortega, N.F. Diseño y análisis de estructuras laminares mediante modelos físicos. Tesis Doctoral. Universidad Nacional del Sur, Departamento de Ingeniería, 1998.
- Paloto J.C., Ortega, N.F. Experimental analysis of acrylic models. Strain, agosto 1998.
- Van Melick, Govaert L.E., Meijer H.E., On the origin of strain hardening in glassy polymers. Polymer 44 (2003) 2493-2502. Elsevier.